Video-Rate Multispectral Infrared Imagery Using Nanostructured Detector-Filter Hybrid Devices

Michael K. Yetzbacher, Heath Gemar, Jerry R. Meyer
Optical Sciences Division, US Naval Research Laboratory
4555 Overlook Ave. SW, Washington, DC 20375

michael.yetzbacher@nrl.navy.mil

ABSTRACT

Emerging nano-scale fabrication technology has strong promise for impacting the battlefield in long-standing problems of spectral sensing. Hyperspectral and multispectral imaging have been used to great effect in military applications. Spectral contrast gives an advantage over panchromatic imaging in detection, identification, and tracking of targets whether performed by AI/machine vision techniques, or by a human observer. Spectral imaging systems are now available at wavelengths of greatest military interest, in the haze-penetrating short-wave infrared and day/night thermal infrared bands. However, the most capable and effective systems are bulky, heavy, and too expensive for wide distribution, deployment on small platforms, or man-portability. In contrast, visible color video systems are at an advanced state, offering desired performance with low size and weight as well as low cost. New color-separation strategies are necessary to allow lightweight, low-bulk, high-capability video systems in the non-visible bands. In particular, nanometer scale, sub-wavelength structures may allow for the miniaturization and low-cost volume manufacturing of multispectral thermal infrared imagers. Here, we present technical details of micro-filter technology for video-rate multispectral and hyperspectral imaging in the visible and short-wave infrared bands and discuss the difficulty of extending this technology into the thermal infrared bands. We further describe research efforts at the US Naval Research Laboratory to design and fabricate nano-structures where the filter and detector are not distinct optical elements due to near-field effects. Such structures may enable video-rate multispectral sensing in the thermal infrared, allowing low-cost, widely distributable day/night spectral video for the warfighter.

1.0 INTRODUCTION

Video-rate infrared imagery is desired in defense applications for imaging moving targets or situational awareness in rapidly changing environments. Spectral imagery is preferred to panchromatic imagery by many human operators, offering additional contrast through spectral differences. When comparable spatial resolution is available, spectral imagery offers advantage over panchromatic imagery in the automated detection/identification of partially obscured targets. While visible-band multispectral imagery is widely available and utilized at all levels, infrared multi-spectral imagery is often only available to the highest priority users due to the size, weight, and power, as well as cost (SWAP-c) required by these systems. Wide distribution of video-rate infrared imagery capability would reduce workload for the highest-demand assets, while giving warfighters a significant advantage in intelligence, surveillance, and reconnaissance.

Visible-band multi-spectral video systems almost exclusively use focal plane division where adjacent pixels are sensitive to different colors arranged in a mosaic array and are repeated as a unit-cell over the entire array. This is commonly known as Bayer pattern filtering, though Bayer is the surname of an inventor of a specific patent for a 2x2 unit cell with diagonal luminance components and two distinct chrominance components. There are now many types of mosaic array filters designed for silicon detectors, some with sensitivity in UV or NIR regions outside the visible band. The mosaic array filter is remarkable in its nearly negligible impact on system SWAP-c while adding color capability. The filter does degrade the spatial resolution of the camera, but image processing can lessen the impact of this spatial resolution loss to an acceptable extent for most applications, especially when the number of bands is low.

The success of the mosaic array in the visible is the result of multiple factors. Overall, the desire for visible-band color imagery is strong. The invention of color photography, more than 160 years ago pre-dates the invention of both photography of moving objects and electric lights. This widespread desire for color imagery meant that at the time of the invention of the digital camera, color motion picture was well-established and expected by consumers. This motivated multi-source, research investment towards digital color video shortly after the invention of the digital camera. The human desire for color was also responsible for an established industry for the production of well-characterized color dyes. Physically, electronic transitions, generally in the visible band, have much stronger dipoles, and therefore absorption coefficients, compared to other transitions in molecules, leading to very strong absorbers in the visible bands. These strong absorbers allowed for effective out-of-band color suppression with very thin absorbing layers, enabling patterning of the filters at the micron scale. This enabled the color mechanism to be negligible in size and weight relative to the camera and there is no additional power requirement other than processing. The focal plane division strategy of the Bayer pattern meant that color sensing is nearly completely separated from the imaging optics, allowing for a modular approach to multispectral systems. Co-fabrication of the mosaic array and sensing array, enabled the cost differential for color and panchromatic systems to approach negligible levels. With no SWAP-c difference, operator preference for color wins out and research was aimed at further eroding the remaining advantage of panchromatic cameras by improvement of demosaicking algorithms to increase mosaic array spatial resolution.

Despite the extensive use of infrared video in the defense industry, technical difficulties have hindered the development of mosaic array filters for multi-spectral infrared video. Due to weaker dipole moments, strong absorbers are not available, so the patterning of a thin layer for a mosaic array using dyes is not possible. Widespread experimentation and multi-source research is not naturally occurring due to the twin financial pressures of much larger cost of infrared sensing arrays and much smaller market for eventual products.

2.0 SEPARATE FILTER FABRICATION

The US Naval Research Laboratory (NRL) has pursued multiple research programs with the goal of enabling low SWAP-c multi-spectral infrared video systems. As industry produces many quality panchromatic infrared imagers, albeit at a high price, the strategy initially focused on fabrication of the mosaic array filter in isolation from the sensing array. Once produced, the mosaic array could be integrated onto a detector array of known grade. A simple strategy of adhesive would be the method of integration. This allows for evaluating the filter quality and yield without destruction of any detectors.

In the absence of strongly absorbing dyes, NRL's Applied Optics Branch pursued a strategy using dielectric filters. Provided appropriately characterized materials, dielectric filters can be designed for any wavelength by substituting materials and scaling the design.

2.1 Reflective Infrared Bands

At room temperature, the light in the band from 900-1700 nm is largely reflected solar light. This short-wave infrared (SWIR) band overlaps with the sensitivity of InGaAs photodiode arrays. NRL partnered with Pixelteq (now Salvo Technologies) to design and fabricate a series of mosaic array filters for the SWIR on pixel pitches of 25 and 12.5 microns with formats matching commercially available cameras. Both 3-band and 9-band versions were produced. In this series of filters, each spectral response of the unit cell was designed completely independently and operated at an F# equal to or greater than 2. Liftoff technique was used to sequentially fabricate the filters. Filter yield through multiple lithography steps was increased by using a non-vertical coating profile. For the 9-band filter, cross-talk from overlapping coatings was reduced by using a 13 micron diameter clear aperture defined with an opaque layer. Figure 1 shows an electron micrograph of the surface of the 9-band filter on the left. Successfully fabricated filters

were integrated onto existing focal plane array sensors by Sensors Unlimited using an active alignment method. The spectral response of the integrated camera using a range including the response of 8 of the 9 bands is shown in Figure 1 on the right.

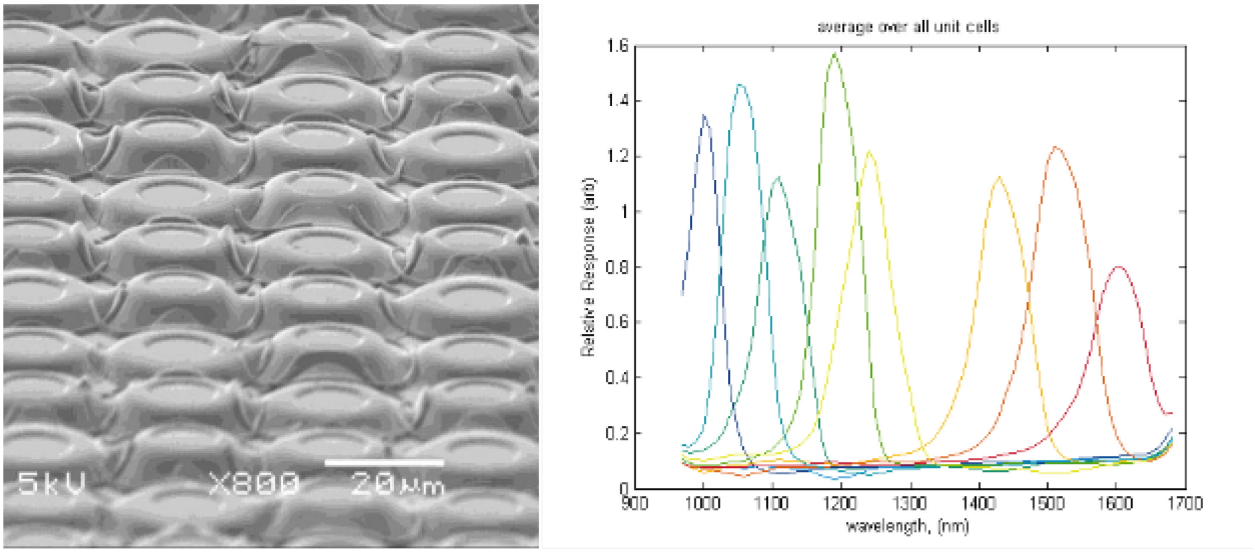

Figure 1: (Left) Electron micrograph of 9-band SWIR filter manufactured by Pixelteq (now Salvo Coatings). Each filter is independently designed and lithographically patterned. (right) spectral response of 8 of the 9 coatings after integration onto the camera. The other band has a spectral peak which is off-scale at lower wavelengths.

The response of the integrated filter and camera is identical to the product of the filter transmission and detector QE above a threshold that is several percent of the peak response. Below this threshold, all channels on the camera are sensitive to light of any wavelength. This cross-talk is likely due to the array modulation transfer function. The camera was designed for general imaging, and cannot distinguish single-pixel illumination to arbitrary contrast. However, the camera has adequate spectral contrast to be used for automated detection and also to display images that show spectral contrast.

As in hyperspectral imaging, the assignment of spectral images in the SWIR or other infrared bands to visible bands for display to a human operator is arbitrary as there is no canonical convention to follow. Images from the 9-band system were often treated with principal components analysis and only displayed using the first few principal components. Images from a 3-band camera where an arbitrary assignment of SWIR bands to red, green, and blue display colors are shown in Figure 2. The photographs were taken of objects slightly more than 1 mile from the rooftop of NRL's DC campus. On the left is an image of refueling tanks and trucks at Reagan National Airport. Note that the SWIR shows color contrast between the white tank which is painted metal and the pink tanks made of plastic which appear white in the visible. In the image on the right, the foliage on the trees shows different colors in the SWIR, possibly giving information about plant species or health.

The capabilities of the 9-band SWIR camera were captured in more detail in another publication [1]. NRL's partners, Salvo Technologies and Sensors Unlimited continue to produce products based on this work, with a standard NIR &SWIR mosaic array camera available as of this writing.

The filter height to pixel pitch ratio demonstrated in this program was as low as 1:4. This is challenging for liftoff lithography of dielectric materials. Future SWIR focal planes are expected to utilize pixel pitches of as small as 5 microns, which is expected to be very challenging for mosaic array filters.

Figure 2: Photographs taken from video recorded with a 3-band SWIR video system. Assignment of SWIR bands to red green and blue display colors has been made arbitrarily. Spectral contrast can be seen in both urban and natural settings. Most of the apparent defocus in the image on the left comes from air turbulence as air is rapidly being heated by the ground. The distance to the object is over 1 mile.

2.2 Thermal Infrared Bands

Thermal infrared bands have wavelengths that are roughly a factor of 4 larger than the SWIR wavelengths. This makes the fabrication of independently fabricated filters prohibitively difficult. Large changes in filter height over short lateral distances cannot be tolerated for dielectric materials. One method that has been proposed to allow for thermal infrared patterned filters is the use of stepped etalons or Fabry-Perot resonators sharing common reflective layers as has been demonstrated in visible bands. Etalons allow for the use of shared non-patterned layers for reflectors. Some Fabry-Perot designs do not have any height differences between filters displaying different spectral responses, but use subwavelength structures to adjust the refractive index within a spacer layer [2]. However, in the simplest design, multi-spectral imaging can be achieved in the thermal infrared using blanket coated few-layer coatings surrounding a single patterned spacer layer. Figure 3 and Figure 4 show a concept of a multi-layer etalon for the mid-wave infrared achievable with only two materials.

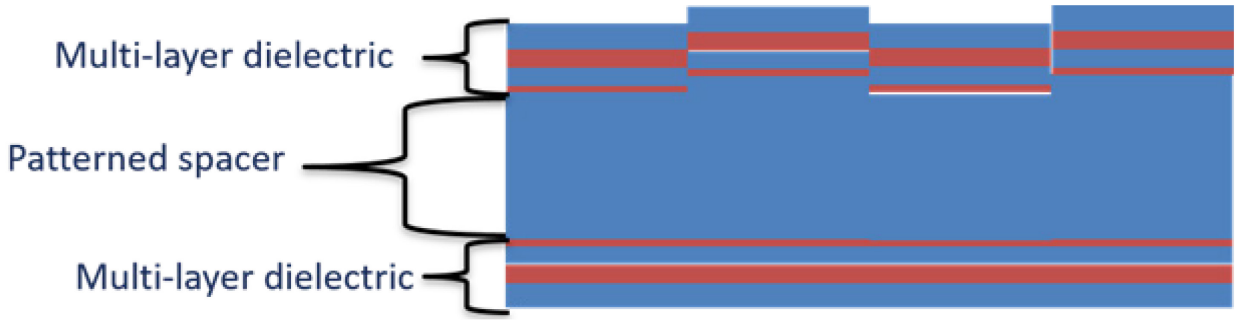

Figure 3: Illustrative cross-section of MWIR multi-level etalon. The patterned etalon can be fabricated on any suitable substrate. Only one patterning step is required. The thickness of the spacer layer determines the spectral sensitivity of each portion of the filter. For a high index spacer layer, less than 350 nm of thickness difference is required to span the 3-5 micron atmospheric transmission band.

The filter presented could be fabricated to provide a MWIR patterned filter using existing techniques with no new technology development. The cross-talk in between the bands could be suppressed by additional unpatterned coatings on the substrate or imaging optics. The low order of the etalons means that the spectral response will not be significantly altered by a large acceptance angle, even using F/1 imaging optics. However, the Lorentzian lineshape inherent in the Fabry-Perot response will limit the number of achievable

bands through cross-talk. The concepts in ref. [3] present a method for recovering pure spectra in the presence of cross-talk using multiple etalon orders. However, for this work, we limit ourselves to simple detection and processing schemes. In this limit, the most viable technologies abandon the separate fabrication of detector and filter elements and use resonant cavities.

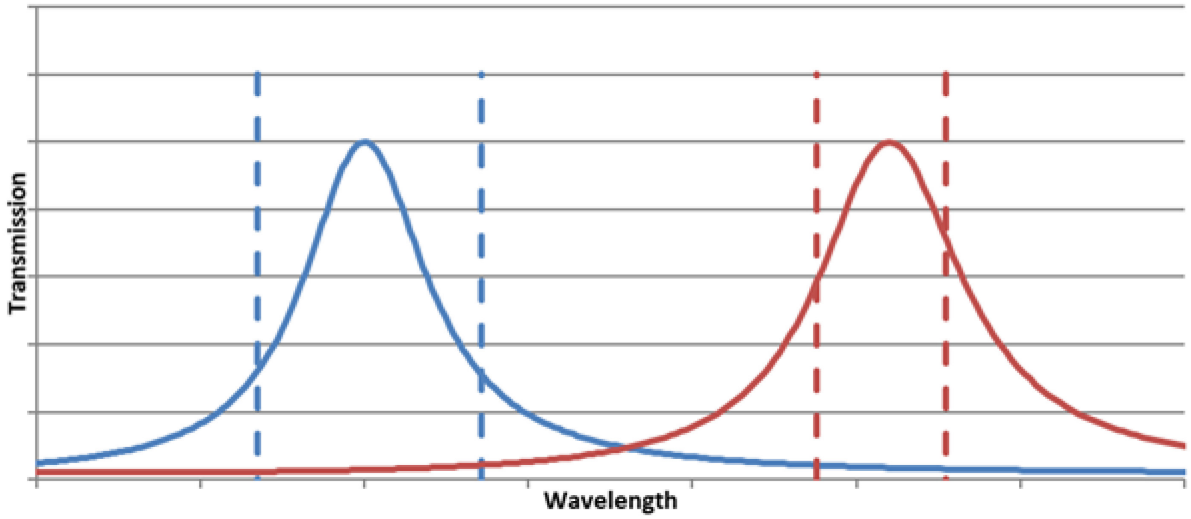

Figure 4: Spectral response as a function of wavelength for second order etalons having a high index spacer with top and bottom reflectors each having a broadband reflectance of 75%. The blue trace has a total etalon thickness of 1 micron and the red trace shows the predicted transmission for an etalon with a thickness of 1.16 microns. Vertical dotted lines represent design goals for sensitivity differential between bands. The total plotted range is within the 3-5 micron wavelength band.

3.0 HYBRID FILTER-DETECTOR DEVICES

In the case of thermal infrared detectors, low bandgap energies mean that the detector dark current may be a significant factor in the detector signal-to-noise ratio. Dark current is independent of the spectral response of the detector, but signal scales with the bandwidth. Spectral separation through filtering input photons reduces signal while noise remains constant. In thermal bands, it is not generally possible to reduce noise, though working toward a thicker detector with higher quantum efficiency as dark current scales with the absorber thickness when the detector is diffusion limited [4]. In MWIR detectors, the specific detectivity, D*, is used as a figure of merit as it includes both sensitivity to signal (or quantum efficiency) and dark current or (noise).

Optical resonance has been used to increase quantum efficiency without increasing dark current. This is done by having the light beam make multiple passes through a thin detector, thereby increasing its effective thickness with respect to signal while the thermally generated noise is a function of the detector volume and not increased by the resonance. The phenomenon of resonance is achieved through constructive interference, and corresponding destructive interference narrows the linewidth, naturally spectrally filtering the detector response. In this case, the filter and detector are not separate elements, but part of the same optical device. The tradeoff for this increased signal-to-noise ratio depends somewhat on the specific type of resonance. Two types of resonant infrared detectors in the MWIR have been recently investigated at NRL.

3.1 Resonant Cavity Infrared Detector (RCID)

Resonant cavity enhanced photodetectors have been known for years, being used for increased detector speed at telecom wavelengths. However, this had not traditionally been exploited to increase the signal-to-

noise ratio of MWIR detectors, or to increase the temperature at which they could effectively operate. In 2019 NRL reported a demonstration of a room-temperature MWIR detector with a D* of 7 x 10^9 cmHz^{½}/W [5]. This specific detectivity is an order of magnitude higher than any previously reported MWIR RCID.

Similar to etalons, the RCID has a Fabry-Perot cavity made by either metal reflectors or a dielectric stack placed on either side of a spacer layer. Unlike the filter illustrated in fig. 2-3, the RCID has a detector layer within the cavity to sample the enhanced fields inside the cavity. The thin absorber layer is responsible for a low dark current and is placed at an antinode where the field is strongest. The thin detector layer is also responsible for extremely fast time response of the detector. An illustration of the necessary components is shown below in Figure 5. Note that optically transparent and conducting components are required on both sides of the detector material.

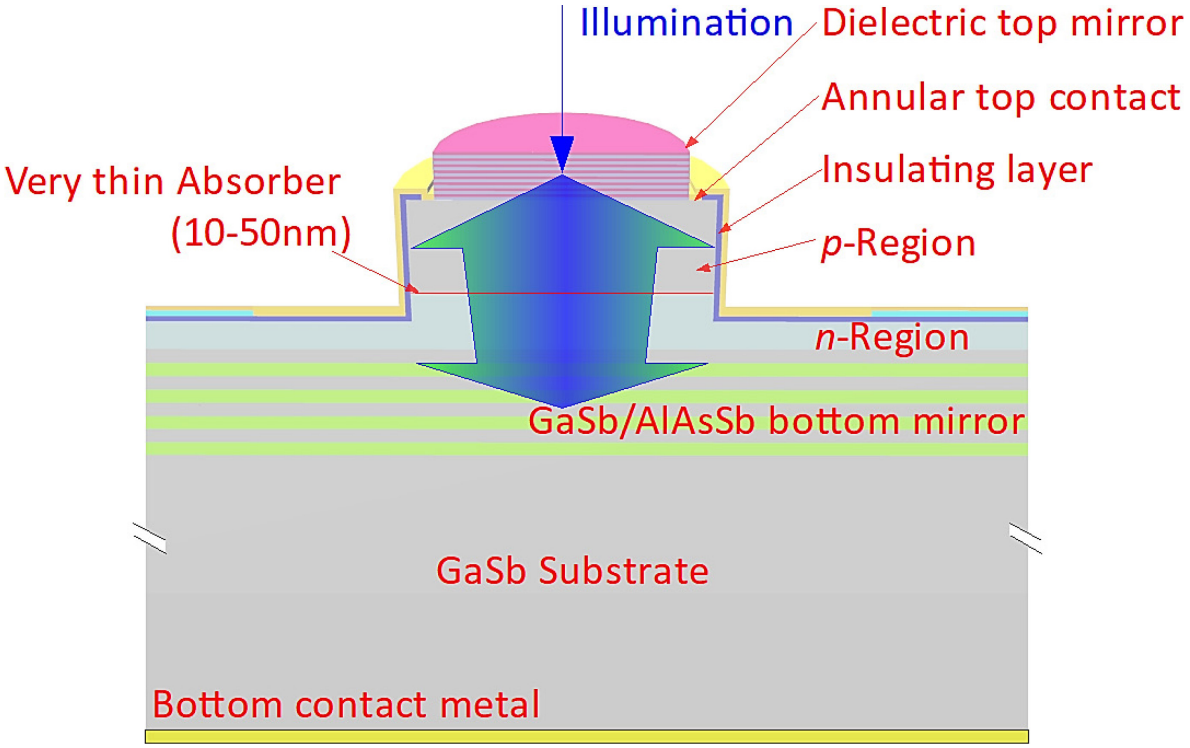

Figure 5: Cross-section diagram of RCID detector. The blue arrows show the light path into and within the cavity. In this example, Bragg reflectors form the top and bottom boundaries of the Fabry-Perot cavity. The increase in D* is due to multiple effects including multiple passes of the field through the detector layer, which has low volume to minimize dark current. The bottom reflector and doped regions and detector structures are grown using molecular beam epitaxy. Precise control over doping levels and thicknesses is required to ensure appropriate reflectivity, precise placement of the absorbing layer, and transparency of materials within the cavity.

When considered as a candidate for MWIR multi-spectral sensing, the RCID has numerous advantages. The necessary trade-off made in an RCID is sacrificing spectral bandwidth for enhanced detectivity. This is precisely the trade system engineers are interested in making for multi-spectral sensing. Figure 6 below shows theoretical calculations of D* as a function of wavelength for a high performance RCID and a conventional detector. The D* achievable with a conventional detector and filter is simply the product of D* for the conventional detector multiplied by the filter transmission, which is guaranteed to suppress D* at unwanted wavelengths, but bring no detectivity enhancement in the desired band. Through the enhanced field interaction with a low-volume absorber, the RCID enhances D*, but only in the spectral region for which it is designed. In the case of broadband reflectors, the peak sensitivity of an RCID can be adjusted

anywhere above the bandgap by adjusting the thickness or the refractive index of the spacer layer. RCIDs with varying spectral response could be fabricated together in a sensing array, though this has not yet been demonstrated.

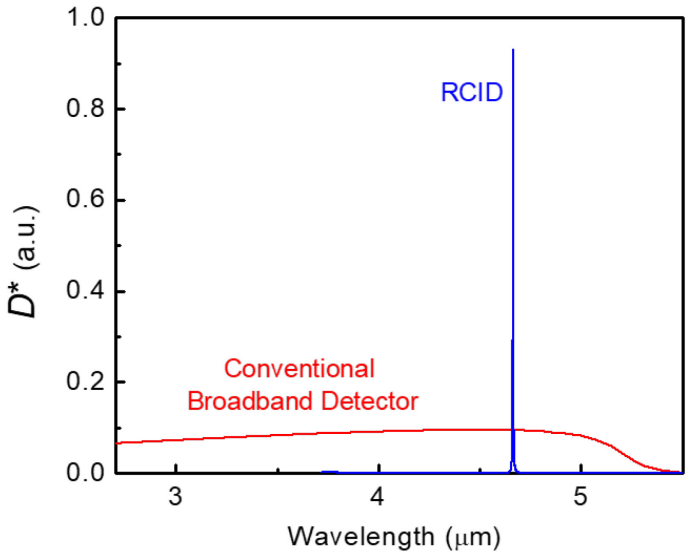

Figure 6: Comparison of the specific detectivity, D*, achievable with a broadband detector (red) and an RCID (blue). The resonance enhancement is necessarily narrow band, but can be substantial and tests at NRL have indicated a resonance enhancement near a factor of 30.

Potential disadvantages of RCIDs are also inherent in Fabry-Perot cavities. The angle of acceptance of a cavity is related to the cavity quality. The resonance enhancement and spectral specificity will not be as strong for very large apertures, due to non-normal incidence light being unable to resonate in the cavity and the response being broadened. However, RCIDs have demonstrated high quantum efficiency at a very respectable F/2 aperture and there is room for improvement in design of mirrors and cavity shapes, as well as minimizing cavity order. RCIDs also are useful for maximizing the opportunity on the smallest platforms, as these systems often are so SWAP constrained they are forced to work with larger F#.

The initial demonstration of high D* MWIR RCIDs by NRL in 2019 made clear that there was substantial room for improvement through material and device optimization. The external quantum efficiency of the initial device was 34%, but more recent work at NRL has resulted in improvements in the external quantum efficiency to 55%. Ongoing studies are investigating the possibility of developing these detectors further for hyper- and multi-spectral imaging, including overcoming some of the challenges involved in making imaging array detectors using RCIDs, and making tunable RCIDs, using microelectromechanical systems (MEMS).

3.2 Resonant Apertures

Other forms of resonant detectors have recently been demonstrated. The phenomenon of extraordinary optical transmission through subwavelength apertures has been known for decades. This phenomenology arises from plasmonic resonances of apertures in metal films. Researchers have suggested this mechanism could be exploited for multi-spectral imaging [6]. However, hurdles to using this technology include the near-field nature of the spectral separation and the incompatibility of broadband detector material with resonance. Proximity of an absorber to the field in an aperture does not allow for resonance, and the phenomenon of spectral separation or enhanced sensitivity is lost. NRL researchers studied this problem, and discovered a way to preserve resonance while detecting the near field.

The basic geometry for the apertures studied is given in Figure 7. The apertures generally have dimensions w<125 nm and h>600 nm. Apertures are designed to be resonant with fields in the 2-5 nm free space wavelength range with electric fields polarized in the x direction. When the apertures are coupled to free space with no near-field absorbing material, the spatial mode of the magnitude of the Poynting field is shown on the left in Figure 8. The node at the center of the y-dimension is due to the magnetic component of the Poynting field. The electric component has the traditional zero-order shape with high magnitude concentrated in the center of the aperture. Introduction of an absorber directly in contact with the metallic layer produces the Poynting field shown in the center of Figure 8, where the mode structure is destroyed and the field magnitude is of the same order as the incident field magnitude. However, the introduction of an isolation layer of approximately 100 nm, restores the resonant field spatial mode and the magnitude of the field within the aperture is again enhanced (see Figure 8, right).

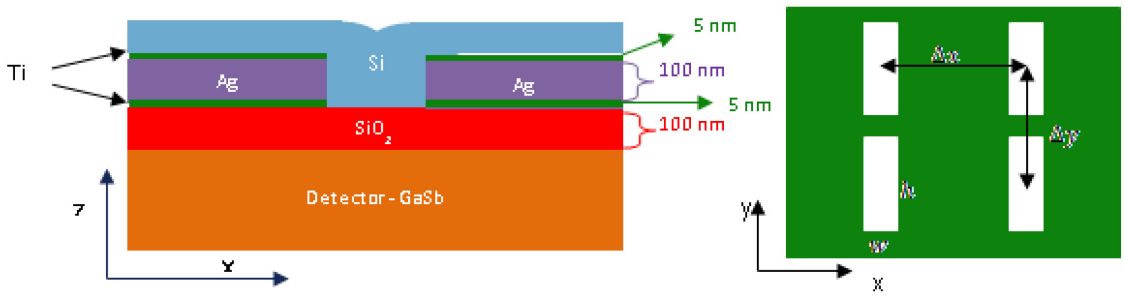

Figure 7: Diagram of resonant apertures coupled to detector material. (Left) Cross-section showing material layers and thicknesses. (right) top view defining the parameters for the apertures with width, *w*, height *h*, and center-to-center distances *Δx* and *Δy*. The apertures repeat in this pattern in the x and y dimensions.

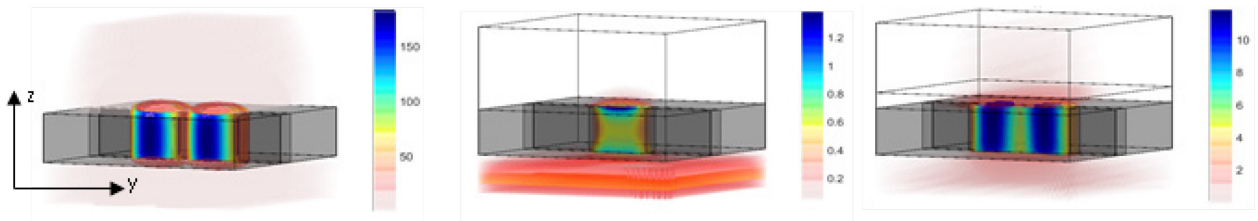

Figure 8: Poynting field magnitude for the rectangular apertures in the MWIR with three different coupling conditions. The gray area represents the metal layers. Left- coupled to vacuum; no surrounding absorbing material. Center – directly coupled to absorbing material at the aperture exit. Right – Weakly coupled to an absorber through a 100 nm spacer layer of silicon dioxide.

The presence of an absorber at any finite distance lowers the cavity quality. An isolation layer is used to control the distance and therefore coupling strength between the cavity and absorber. The absorber has the expected effect on the resonance bandwidth but also, when the absorber functions as a detector, the isolation layer has an effect on the quantum efficiency of the detector. This is due to a tradeoff between two effects of spatial overlap between the evanescent cavity field and the absorber material, resulting in greater coupling due to spatial proximity of the evanescent field and lower cavity quality due to losses from the absorber material. The results of a study of an evaluation of cavity quality and quantum efficiency are shown below in Figure 9. The cavity quality increases with increasing isolation layer thickness, as expected. In the plot on the right of Figure 9, it can be seen that the cavity quality and enhanced field effects dominate at distances out to about 100 nm, and then the spatial overlap between the absorber and cavity field becomes the dominant effect. This means that optimal quantum efficiency is reached where these two effects balance each other out, near 100 nm of isolation layer thickness. Additional details about the calculations are presented in ref. [7].

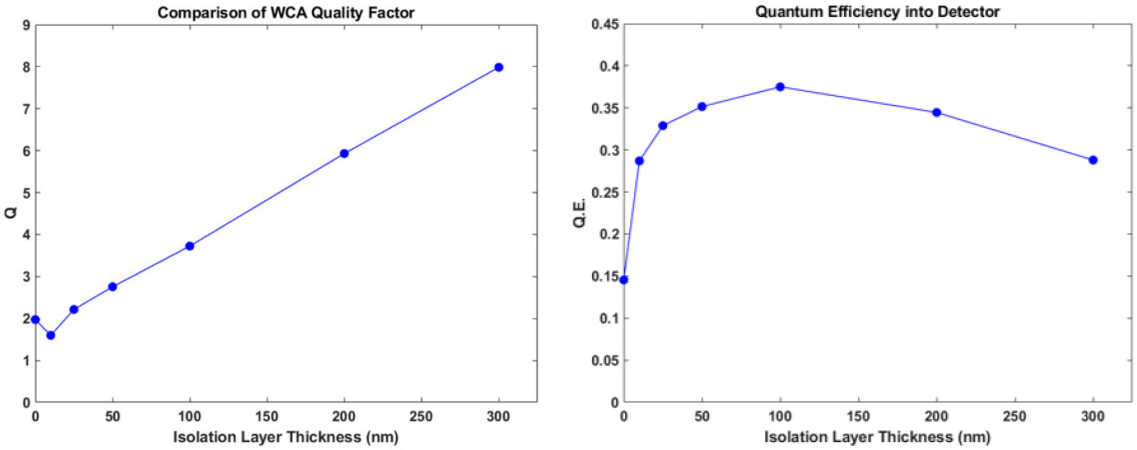

Figure 9: Result of simulations of cavity and detector properties with increasing isolation layer thickness. Left – cavity quality, Right – detector external quantum efficiency.

Apertures were fabricated using the materials and thickness dimensions shown in Figure 8. Detectors with resonant apertures were fabricated at several different lateral aperture dimensions. In general, the detectors all displayed spectral sensitivity. One plot of spectral response is shown in Figure 10 along with a simulation of the fitted spectral response from the device. The device response was different than designed being both blue-shifted and broader than the initial design. This is likely due to incomplete fill of the aperture with the silicon fill material. However, good agreement is regained when the fill material is reduced to 8% of the aperture volume-index product. Additional research is needed to better control the effective refractive index of the aperture and enable design control.

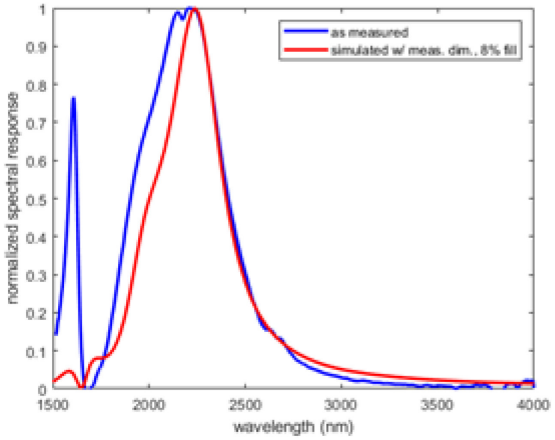

Figure 10: Measured response (blue) and simulated response (red) from a cavity having plasmonic resonance weakly coupled to absorbing material which is monitored as a detector. This is the first demonstration of detector-coupled extraordinary optical transmission.

Though the research on resonant aperture detectors is early stage, there are characteristics of these detectors that suggest this class of detector may outperform all others for multi-spectral imaging. Resonant aperture detectors are quite insensitive to the incidence angle of the incoming beam. This allows them to be used with state-of-the-art high-aperture lenses, leading to greater sensitivity. The enhanced fields should allow for detector layers to be made very thin, reducing dark current. Additionally, these detectors have the capability to enable spectral imaging with much greater efficiency. One drawback of the focal plane division strategy

used for multi-spectral video is the tradeoff required between spatial and spectral resolution. That is, for each band, some position on the focal plane array is required, not allowing for measurement of additional spatial information at that focal plane location. Current basic research at NRL seeks to overcome this tradeoff, by allowing detectors to have overlapping areas of spatial sensitivity using resonant apertures.

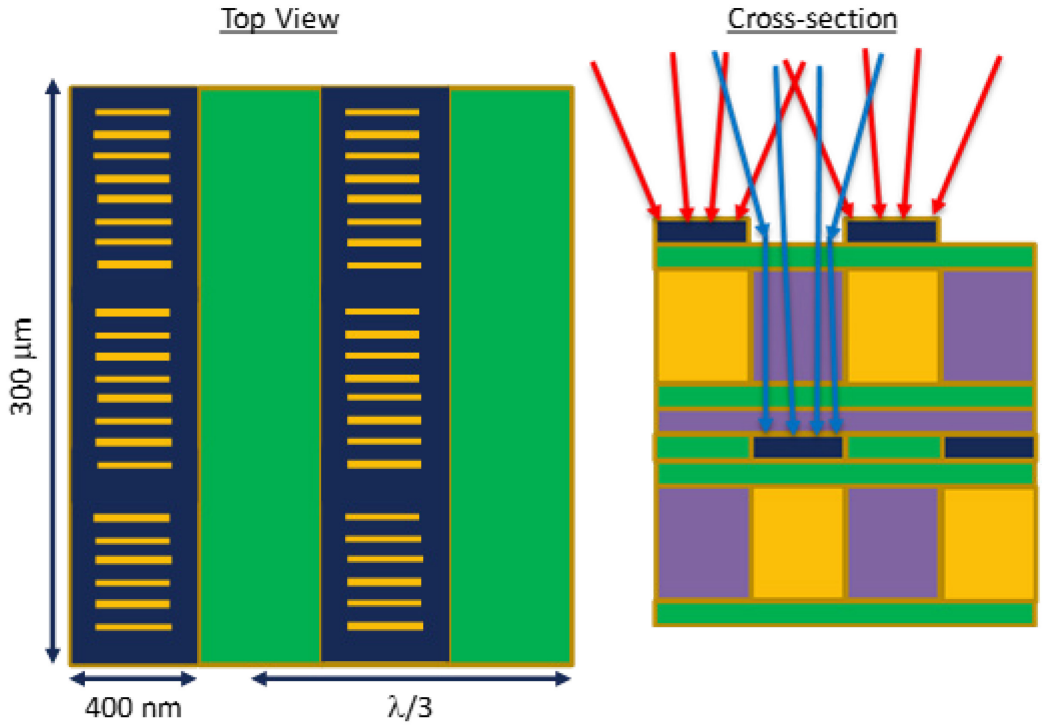

Figure 11: Concept of multi-spectral detector sampling the same spatial region of optical fields with different spectral sensitivities. Apertures in the dark blue metal layers can be tuned independently and coupled to distinct detectors (in gold). Due to the contact requirements for detection, conducting and transparent layers (in green) and insulating transparent layers (in purple) are required.

Current calculations indicate that the spatial sensitivity of resonant apertures is larger than their physical size. An aperture that is of the order of 1/30 of the wavelength samples fields that are of the order of 1/3 of the wavelength. This is a factor of 10 in the difference between physical and optical extent. It is therefore possible to have different resonant apertures coupled to different detectors and sampling the same spatial area for the optical field. A concept of a detector having two spectrally independent outputs from optically overlapped fields is presented in Figure 11. The apertures on the upper level are resonant with one wavelength, while apertures on a lower level are sensitive to a different wavelength. The apertures "funnel" the light from a broader area, and are able, in theory, to be 100% efficient. However, much research remains to determine how much of the light funneling will be practical in a multi-level device with multiple index boundaries.

4.0 SUMMARY

Video-rate multi-spectral imaging in the infrared is possible, and may be able to be widely distributed by low-cost volume manufacturing in the foreseeable future. For the SWIR band, technology is relatively mature, and vendors with appropriate capability exist. In the MWIR, limited capability is currently available. Low-order etalons multi-spectral systems can be rapidly fabricated and deployed, but do not demonstrate

capability for expansion of the number of bands or meeting the imaging performance of panchromatic systems. Two technologies exist that may enable very high performance MWIR systems. RCIDs have been demonstrated with enhanced D*, but require further development into array and/or tunable systems. Resonant apertures have been demonstrated which have shown spectral sensitivity. This class of detector has the potential for full utilization of incident photons through spectral funneling, but this has not yet been demonstrated.

5.0 REFERENCES

[1] "Video rate nine-band multispectral short-wave infrared sensor", Kutteruf, MR.; Yetzbacher, MK.; DePrenger, MJ.; Novak, KM;. Miller, CA; Downes, TV; Kanaev, AV. Applied Optics Volume: 53 Issue: 13 Pages: C45-C53 Published: May 1 (2014).

[2] "Broadband tunable, narrow linewidth multispectral color filter", Xiang, J; Song, M; Zhang, Y; Kruschwitz, J; Cardenas, J, Frontiers in Optics + Laser Science 2022 (FIO, LS), Technical Digest Series (Optica Publishing Group, 2022), paper FM5D.3.

[3] "An analytic method for spectrum recovery from wedge or staircase spectrometers" By: Yetzbacher, Michael K.; Miller, Christopher W.; DePrenger, Michael J. Conference: Conference on Next-Generation Spectroscopic Technologies XI Location: Orlando, FL Date: APR 16-18, 2018 Sponsor(s): SPIE Next-Generation Spectroscopic Technologies XI, 2018 Book Series: Proceedings of SPIE Volume: 10657 Article Number: UNSP 106570F Published (2018).

[4] "Interpreting mid-wave infrared (MWIR) HgCdTe photodetectors," Tennant, WE, Prog. Quantum Electron. v.36(2-3), 273–292 (2012).

[5] "Resonant-cavity infrared detector with five quantum-well absorber and 34% external quantum efficiency at 4 μm", Canedy, CL; Bewley, WW; Merritt, CD; Kim, CS; Kim, Warren, MV; Jackson, EM; Nolde, JA; Affouda, CA; Aifer, EH; Vurgaftman, I; Meyer, JE, Optics Express, v.27, no. 3 (2019).

[6] "Planar, Ultrathin, Subwavelength Spectral Light Separator for Efficient, Wide-Angle Spectral Imaging", Buyukalp, Y; Catrysse, PR; Shin, W; Fan, S, ACS Photonics, v.4, p.525 (2017).

[7] "Near-field coupling of absorbing material to subwavelength cavities", Gemar, H; Yetzbacher, MK; Driggers, RG; Renshaw, CK, Optical Materials Express, v.11 no.8, p. 2576 (2021).